Talanta 103 (2013) 228–235

Contents lists available at SciVerse ScienceDirect

Talanta

journal homepage: www.elsevier.com/locate/talanta

Amperometric glucose biosensor based on electroconductive hydrogels

Christian N. Kotanen [a,b], Chaker Tlili [a,c], Anthony Guiseppi-Elie [a,b,c,d,e,*]

[a] Center for Bioelectronics, Biosensors and Biochips (C3B), Clemson University Advanced Materials Center, 100 Technology Drive, Anderson, South Carolina, SC 29625, USA
[b] Department of Bioengineering, Clemson University, Clemson, South Carolina, SC 29634, USA
[c] Department of Chemical and Biomolecular Engineering, Clemson University, Clemson, South Carolina, SC 29634, USA
[d] Department of Electrical and Computer Engineering, Clemson University, Clemson, South Carolina, SC 29634, USA
[e] ABTECH Scientific, Inc., Biotechnology Research Park, 800 East Leigh Street, Richmond, Virginia, VA 23219, USA

ARTICLE INFO

Article history:
Received 19 August 2012
Received in revised form
10 October 2012
Accepted 11 October 2012
Available online 1 November 2012

Keywords:
Biofabrication
Biotransducers
Biosensors
Amperometry
Hydrogels
Glucose oxidase
Glucose
Membranes

ABSTRACT

Fabrication of an enzyme amperometric biosensor for glucose via electropolymerization of pyrrole in the presence of glucose oxidase onto a hydrogel coated platinum electrode is hereby established as a viable biotransducer fabrication method. Platinum micro- (ϕ=25 μm) and macro- (ϕ=100 μm) electrodes were electrochemically activated and chemically modified with 3-aminopropyl-trimethoxysilane (APTMS), functionalized with acryloyl(polyethyleneglycol)-N-hydroxysuccinamide (ACRL-PEG-NHS), dipped into a polyHEMA based hydrogel cocktail and UV cross-linked. Electropolymerization of Py in the presence of GOx produced glucose responsive biotransducers that showed; (i) a 4-fold reduction in sensitivity compared with directly electropolymerized PPy films, (ii) an electropolymerization charge density dependence of biotransducer sensitivity and enzyme activity that was maximal at 1.0 mC/cm^2 with an apparent K_M of 33 mM, (iii) interference screening of ascorbic acid and (iv) a temporal increase in sensitivity with storage over a 17 days period. This method has the ability to precisely and quantitatively add enzyme catalytic bioactivity to metal or semiconductor biointerfaces for applications in biosensors, bioelectronics and bionics.

1. Introduction

Enzyme amperometric biosensors for glucose continue to receive considerable attention because of their critical role in clinical chemistry, particularly the monitoring of glucose levels of diabetic patients, in biotechnology, and in the food industry [1,2]. Recently, a new application of the glucose biosensor was developed [3]. Glucose, along with lactate, are key metabolites whose real time and temporal levels are crucial for the management of hemorrhagic shock; a condition that can lead to multiple organ dysfunction syndrome and/or eventual death [4]. To increase the survival rate of injured patients at risk for hemorrhagic shock, it is imperative that we develop a simple, rapid, sensitive, continuous and selective on-site platform that can quantify glucose levels; identified as a trauma-related biomarker because of its relation to insulin resistance [5–7] and its physiologic link to lactate via the *Cory Cycle*. The continuous monitoring of glucose levels in severely injured patients becomes significant in evaluating the severity of injury and understanding the temporal progress towards hemorrhagic shock with the view to helping the intensivist optimize resuscitation and reanimation [8].

To meet the requirements of dual analyte biosensing of glucose and lactate using micron-dimensioned microfabricated electrodes [9], the biofabrication technique must immobilize the different enzymes at the surface of adjacent electrodes on a monolithic transducer substrate. Various immobilization procedures are possible; including entrapment and encapsulation [10,11], covalent coupling [12,13], cross-linking [14,15], physical–chemical adsorption [16–18] and photolithographic patterning [19]. The simultaneous guiding and immobilization of the enzyme glucose oxidase via the process of electropolymerization of pyrrole into an electropolymerized polymer membrane is an attractive method for the electrode specific immobilization of glucose oxidase and other enzymes [11,20,21]. Other benefits of polypyrrole include efficiency of enzyme loading, ease of preparation, stability of the PPy film at ambient condition and control of the exact amount of immobilized enzyme via the electropolymerization charge density used to create the PPy/enzyme composite film thickness. However, such immobilized enzymes rapidly lose their activity due to denaturation and/or leaching [22]. The simultaneous guiding and immobilization of the enzyme via the process of electropolymerization of pyrrole to form an electropolymerized polymer *within* an existing electrode-supported, swollen hydrogel membrane layer is an area of pioneering investigation by our group.

In this paper we describe further the process, introduced earlier [23–26], of electropolymerization of pyrrole within hydrogel-coated

* Corresponding author at: Center for Bioelectronics, Biosensors and Biochips (C3B), Clemson University Advanced Materials Center, 100 Technology Drive, Anderson, South Carolina, SC 29625, USA. Tel.: +1 864 656 1712; fax: +1 864 656 1713.
E-mail address: guiseppi@clemson.edu (A. Guiseppi-Elie).

0039-9140/$ - see front matter © 2012 Elsevier B.V. All rights reserved.
http://dx.doi.org/10.1016/j.talanta.2012.10.037

microelectrodes to form an enzyme/PPy/hydrogel composite membrane we call a bioactive electroconductive hydrogel. Reported here is the influence of electropolymerization charge density (mC/cm^2), used as a means for increasing enzyme loading and optimizing amperometric bioanalytical performance, such as response time, sensitivity and limit of detection. Also reported are the influence of electropolymerization charge density on immobilized enzyme kinetics and the storage stability of the resulting glucose biosensors.

2. Experimental

2.1. Chemicals and reagents

Pyrrole monomer (reagent grade 98+%), Glucose oxidase (GOx, E.C. 1.1.3.4 from *Aspergillus niger*), 2-hydroxyethyl methacrylate (HEMA), tetra(ethylene glycol) diacrylate (TEGDA, technical grade), poly(ethylene glycol) (400)monomethacrylate (PEGMA), *N*-[Tris-(hydroxymethyl)methyl]acrylamide (HMMA, 93%), polyvinylpyrrolidone (pNVP, MW=360,000), 2-(Dimethylamino)ethyl methacrylate (DMAEMA, 98%), the photo-initiator 2,2-Dimethoxy-2-phenylacetophenone (DMPA, 99+%), β-D(+)-glucose, ascorbic acid, sodium dihydrogen phosphate, disodium hydrogen phosphate, potassium chloride, sodium hydroxide, and sulfuric acid were purchased from Sigma Aldrich Co. (St. Louis, MO, USA). 2-(Methacryloyloxy)ethyl 2-(trimethylammonio) ethyl phosphate (MPC) was purchased from Tokyo Chemical Industry CO., Ltd. The HEMA, methacrylate and diacrylate reagents were passed through an inhibitor removal column (Sigma-Aldrich) for removal of the polymerization inhibitors hydroquinone and monomethyl ether hydroquinone before using them in the preparation of the hydrogel cocktail. Pyrrole monomer was purified by double passage over an alumina silicate column. Solutions were prepared in deionized water prepared by purifying distilled water through a Milli-Q® plus (Millipore Inc.) ultrapure water system. The glucose stock solution of 1.0 M was prepared and allowed to mutarotate overnight.

2.2. Electrochemical measurements

Electrochemical experiments were performed using a BAS-100B/W Electrochemical Analyzer with a BAS PA-1 preamplifier module used to amplify the current and to filter out noise (BAS, West Lafayette, Indiana, USA). All experiments were carried out in a three-electrode setup with platinum microelectrodes(ϕ=25 μm or 100 μm; BAS) as the working electrode, a Ag/AgCl (3 M KCl) reference electrode (RE803; ABTECH Scientific, Inc., Richmond, Virginia, USA) and a platinum mesh counter electrode.

2.3. Preparation of the enzyme electrodes

A 3 mol% TEGDA cross-linked standard hydrogel cocktail was prepared according to a previously described recipe and protocol [27] by mixing HEMA, TEGDA, PEG(400)MA, MPC, HMMA, p(NVP), DMAEMA, and DMPA in typical ratio 78:3:5:1:5:2:5:1 mol%. A 1:1 (v/v) solution of ethylene glycol/water corresponding to 20% of the volume of the monomer cocktail was then added and the mixture stirred overnight under UV-free conditions. Initially, the working platinum macroelectrode (BAS, ϕ=100 μm) was mechanically polished with 0.05 μm alumina for 10 min and then washed with nanopore water and acetone, respectively, in order to expose a fresh platinum surface. The electrode was then immersed in 0.5 M sulfuric acid, made the working electrode of a three electrode electrochemical cell and was electrochemically cleaned by sweeping the potential between −0.20 and 1.40 V (*vs.* Ag/AgCl, 3 M KCl) at 100 mV/s until a steady state cyclic voltammogram was obtained. This electrochemical pretreatment was followed by rinsing with nanopore water several times to ensure good repeatability of electrode surfaces. Following cleaning the bare platinum microelectrode surface was silanized by incubation in a 0.1 wt% solution of 3-aminopropyltrimethoxysilane (APTMS) in anhydrous toluene for 1 h followed by thorough rinsing with toluene and water. The electrode surface was subsequently functionalized with acrylate groups by incubation in a solution of 1 m Macryloyl(polyethyleneglycol)-N-hydroxysuccinamide (ACRL-PEG-NHS, MW 400) in 0.1 M HEPES buffer, pH=8.5 for 2 h. Functionalization of electrodes was followed by ultrasonication in Milli-Q®water for 5 min and drying with ultrahigh purity nitrogen.

Immediately following cleaning, surface modification and PEG-ACRL functionalization, the bare platinum microelectrode was dipped into the 3 mol% TEGDA cross-linked p(HEMA)-based hydrogel cocktail which had been sonicated and sparged with nitrogen. The thin film was then crosslinked with UV light for 5 min using a UV cross-linker (CX-2000 Crosslinker, UVP, Upland, CA, USA) under an inert nitrogen atmosphere to yield a hydrogel membrane that was approximately 5 μm thick.

Electropolymerization of pyrrole was used as the principal means for bioimmobilization of the enzyme on the hydrogel-modified microelectrode [26]. Before electropolymerization of pyrrole, the hydrogel modified electrode was immersed and incubated in 5.0 ml of an aqueous Py (0.4 M)/GOx(1 mg/ml) solution, pH=6.0, prepared in Milli-Q®water for 1 h to ensure equilibrium between the hydrogel film and the electropolymerization solution. Finally, potentiostatic electropolymerization was commenced by the application of 0.75 V *vs.* Ag/AgCl, 3 M KCl to the Pt W.E. leading to polypyrrole formation within the hydrogel membrane [28] and the concomitant immobilization of GOx within the hydrogel. This produced an enzyme-loaded, electroconductive polymer PPy-hydrogel composite (PPy–GOx-Gel|Pt). The enzyme electrode was subsequently washed with Milli-Q®water and by PBS to remove any unbound GOx from the hydrogel film. Electropolymerization charge densities of 0.1–100 mC/cm^2 were explored.

2.4. Characterization of electrodes and enzyme electrodes

Microelectroes were characterized at various stages of fabrication, including cleaned and APTMS surface modified, using the probe 50 mM $Fe(CN)_6^{3-/4-}$ and in ferrocene monocarboxylic acid (FcCOOH). Before use, enzyme-modified microelectrodes were over-oxidized (OPPy) by repeatedly cycling the electrode in PBKCl (100 mM, pH 7.0) between 0 and 1.2 V *vs.* Ag/AgCl, 3 M KCl for 40 cycles at 100 mV/s. For immobilized enzyme kinetics, biosensor sensitivity, response time and biosensor stability studies, amperometric measurements were performed at 0.4 V *vs.* Ag/AgCl, 3 M KCl and by sequential injection of appropriate aliquots of glucose solution into 5.0 ml of 100 mMPBKCl (pH 7.0) under continuous stirring to provide for convective transport.

3. Results and discussion

3.1. Preparation and characterization of microdisc electrodes

Platinum microdisc electrodes were cleaned, surface modified with APTMS (APTMS|Pt) and then chemically functionalized with PEG-ACRL (|ACRL-PEG|APTMS|Pt) for the eventual attachment of the bioactive hydrogel membrane layer and subsequent electropolymerization of Py to simultaneously immobilize the enzyme, GOx, within the hydrogel membrane layer. To confirm the adsorption of the silanol layer of primary amines on the

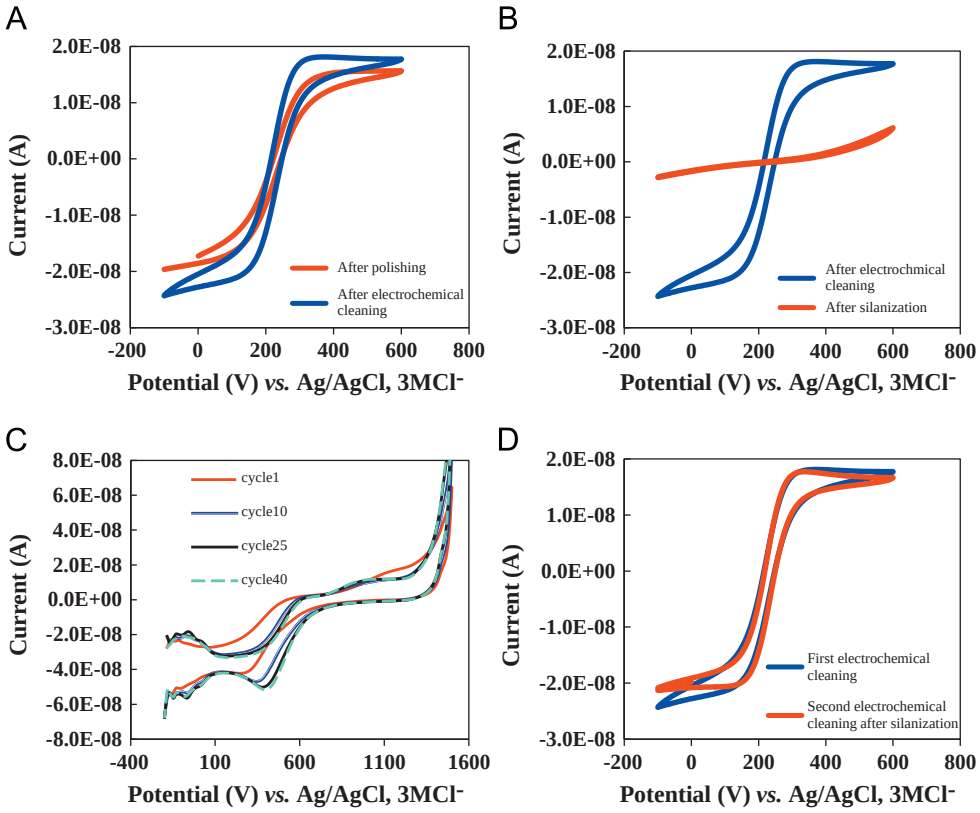

Fig. 1. Cyclic voltammograms of the Pt-ME (ϕ=25 μm) in 10 mM PBS at pH 7.0 in the presence of 5 mM $Fe[CN]6^{3-/4-}$. (A) A direct comparison of an alumina polished electrode (red) with one electrochemically cleaned in 0.5 M H_2SO_4 by repeated cycling over the range −0.2 to 1.5V *vs.* Ag/AgCl, 3M Cl^-at 100 mV/s (blue). (B) A comparison of electrochemically cleaned electrode (blue) with one that was surface modified by APTMS (red, APTMS–Pt). (C) Multiple cycles associated with electrochemical cleaning. (D) A comparison of an electrochemically cleaned electrode (blue, |Pt) with an electrode that was surface modified with APTMS (red, APTMS–Pt) and subsequently electrochemically cleaned as in A above. (For interpretation of the references to color in this figure legend, the reader is referred to the web version of this article.)

microelectrodes, following solvent cleaning and surface modification by APTMS, electrodes were analyzed by cyclic voltammetry in 1:1 50 mM $Fe(CN)_6^{3-/4-}$. Following electrochemical cleaning in 0.5 M H_2SO_4 by repeated cycling over the range −0.2 to 1.5 V (100 mV/s)*vs.* Ag/AgCl, 3 M Cl^-, electrodes were again characterized in 1:1 50 mM$Fe(CN)_6^{3-/4-}$. Fig. 1 shows the voltammograms that were obtained for ϕ=25 μm) Pt-ME.

Panel A of Fig. 1 shows that the electrochemical cleaning protocol improves the microelectrode characteristics in $Fe[CN]6^{3-/4-}$; producing a voltammogram that approaches microelectrode ideality. Panel B shows the result of APTMS silanol surface modification to be a passivated microelectrode with little access of the redox couple to the electrode. Panel C shows the application of 40 cleaning cycles over the range −0.20 to 1.50 V (*vs.* Ag/AgCl, 3 M KCl)at 100 mV/s until a steady state cyclic voltammogram was obtained. Panel D shows the result of the characterization repeated following the electrochemical cleaning protocol to return the electrode to a condition similar to the originally cleaned ideal microelectrode behavior.

Fig. 2 shows the effect of this electrochemical cleaning protocol on the electrochemical behavior of the probe molecules, $Fe(CN)_6^{3-/4-}$ and FcCOOH, at the electrochemically cleaned and as-modified Pt macrodisc electrode Pt-ME (ϕ=100 μm).

Panel A of Fig. 2 shows a modest increase in the peak potential of the APTMS surface modified Pt macroelectrode compared to cleaned bare electrode in the $Fe(CN)_6^{3-/4-}$ redox system. At a pH of 7 it is expected that the immobilized amine functional groups of the APTMS chemisorbed layer will carry some fraction of associated positive charges [29]. The electrostatic attraction of APTMS is likely increasing the electrode boundary concentration of the negatively charged $Fe(CN)_6^{3-/4-}$ causing the observed increase in peak oxidation reduction current. The shift in the reduction potential for the $Fe(CN)_6^{3-/4-}$ can be expected for the APTMS coated electrode as it is less likely to transfer electrons to the higher concentration of negatively charged ferricyanide in conjunction with electrophilic tertiary amine groups at the electrode surface. The system with ferrocene monocarboxylic acid did not show any peak shifts or changes in peak currents, but rather generated similar currents with the APTMS electrode when compared to the bare electrode. Most important however is the implication that on the microelectrode scale the chemisorbed silanaol layer is contiguous and passivating while on the macroelectrode scale the chemisorbed layer lacks the integrity to serve as a passivation layer and is likely discontinuous and establishes that at Pt-ME (ϕ=100 μm) redox active molecules can gain access to the macroelectrode surface.

3.2. *Response to H_2O_2*

The dose-response performance of the bare platinum microdisc electrode (|Pt) and the APTMS modified macroelectrode (APTMS|Pt) were each evaluated for their electrochemical discharge of hydrogen peroxide, the active source of electrons in Generation I amperometric enzyme biosensors of the type investigated following. Fig. 3 shows the performance of the bare macroelectrode (|Pt) and the APTMS modified macroelectrode (APTMS|Pt) to H_2O_2 revealing a sensitivity of 11.5 μA/μM/cm^2 and 0.5 μA/μM/cm^2 respectively; a decrease of nearly two orders of magnitude. These results would indicate that the surface modification procedures, while producing a discontinuous layer on the electrode, nonetheless influences the sensitivity of the

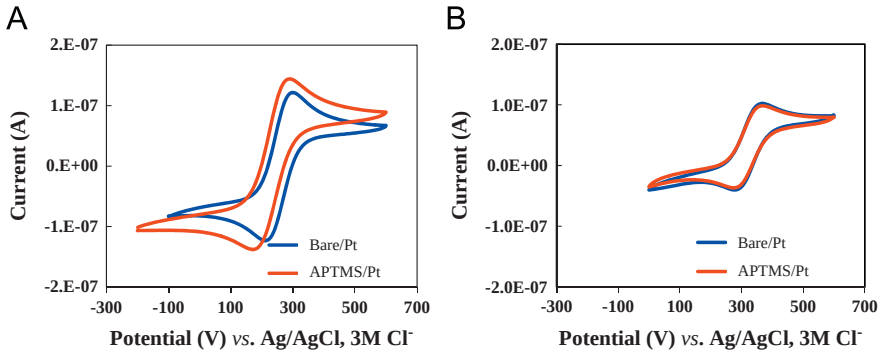

Fig. 2. Cyclic voltammograms of the Pt-ME (ϕ=100 μm). (A) A comparison of an alumina polished and electrochemically cleaned electrode (blue, |Pt) with one that was surface modified with APTMS (red, APTMS–Pt) as tested in 10 mM PBS at pH 7.0 in the presence of 5 mM $Fe[CN]_6^{3-/4-}$. (B) A comparison of an alumina polished and electrochemically cleaned electrode (blue, |Pt) with one that was surface modified with APTMS (red, APTMS–Pt) as tested in 10 mM PBS at pH 7.0 in the presence of 5 mM FcCOOH. (For interpretation of the references to color in this figure legend, the reader is referred to the web version of this article.)

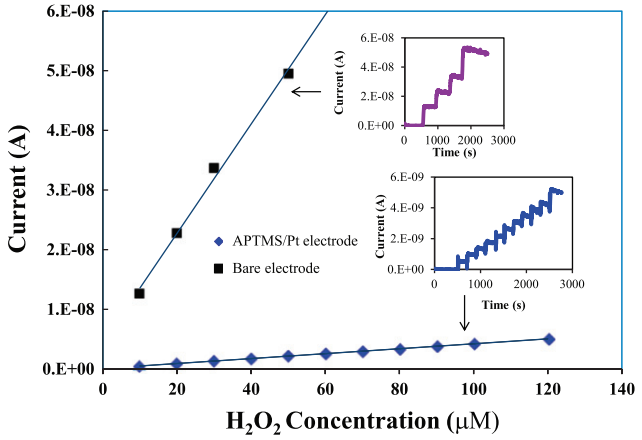

Fig. 3. Dose-response curves for Pt-ME (ϕ=100 μm) that were electrochemically cleaned (|Pt) and modified with APTMS (APTMS–Pt) as tested in 10 mM PBS at pH 7.2 in the presence of varying concentration of H_2O_2.

biotransducers to H_2O_2, which may be due to the blocking of charge transfer sites by the APTMS layer and the addition of a diffusional barrier [30]. This change in response to $H_2O_2$is more pronounced compared to the other electrochemically active species of FcCOOH and $Fe(CN)_6^{3-/4-}$ that appear to not be blocked by APTMS.The amperometric detection of H_2O_2 in this experiment was performed at 400 mV *vs.* Ag/AgCl, while electrochemical oxidation of hydrogen peroxide at metallic electrodes is typically done at 600 mV *vs.* Ag/AgCl [31]. The electron transfer rate constants for oxidation of FcCOOH and H_2O_2 are $2.2\times10^5\ M^{-1}\ s^{-1}$ at platinum electrodes [32] and $4\times10^2\ M^{-1}\ s^{-1}$ at Prussian Blue modified electrodes respectively [33]. Because of the high second-order homogeneous rate constant of FcCOOH and the lack of perturbation to the voltammogram of FcCOOH after APTMS electrode modification, a change in diffusivity is likely not the cause of the decreased current response to H_2O_2. For these reasons we believe that the APTMS modification may be leading to a decrease in the oxidative electron transfer rate constant of H_2O_2 in some fashion other than contributed by a change in diffusivity. Differences in adsorption of FcCOOH, $Fe(CN)_6^{3-/4-}$ and H_2O_2 into the APTMS layer may also be the cause.

3.3. *Bioanalytical performance of the immobilized GOxbiotransducers*

Following hydrogel casting, the immobilized enzyme electrodes were prepared by electropolymerization of pyrrole in the presence of GOx leading to entrapment of GOx within the hydrogel and the fabrication of a bioactive, electroconductive hydrogel. The preparation of glucose responsive biotransducers by the immobilization of GOx via electropolymerization of Py is well documented in the literature [23,24,34–37]. Firstly, a comparison was made of the performance of biotransducers prepared using the current hydrogel method with that prepared by the previously established method. Fig. 4A shows the dose-response curves obtained for systems of PPy–GOx|Pt and PPy–GOx-Gel|Pt where the former was prepared by the electropolymerization of Py in the presence of 1.0 mg/ml GOx at a cleaned and unmodified electrode and the latter was prepared by the electropolymerization of Py in the presence of 1.0 mg/ml GOx at a hydrogel-coated (ca. 5.0 μm) electrode. Both biotransducers were prepared using a charge density of 10.0 mC/cm^2. Biotransducers showed monotonically increasing current responses to infusions of glucose. The chronoamperometric response was stable under gentle stirring conditions with steady state currents being reached and maintained at response times ranging from 10 to 70 s. It is clear that the non-hydrogel system displays a fourfold higher sensitivity (50 pA/mM) compared to the hydrogel modified biotransducer (12 pA/mM). Secondly, the hydrogel modified biotransducer displays a change in slope and thus shows two linear regimes. Secondly, a comparison was made of the performance of biotransducers prepared by the current hydrogel method when using different electropolymerization charge densities, Fig. 4B. The bioanalytical performance of the various transducers studied is summarized in Table 1.

Hydrogels of implantable biotransducers are a needed component for conferring their ability to impart biocompatibility through reduction in protein fouling [27], reduction to the inflammatory and foreign body responses [38], and reduction to fibrous encapsulation [4]. The response of the freshly prepared (10 mC/cm^2) glucose biosensors based on PPy–GOx-Gel|Pt composite was linear over the range 1–6 mM, with a sensitivity of 153 $nA/mM/cm^2$ and a response time of 25 s. The sensitivity of the freshly prepared (10 mC/cm^2) glucose biosensor without hydrogel film (PPy–GOx|Pt) was linear in the range 1–10 mM with a sensitivity of 637 $nA/mM/cm^2$ and a response time of 18 s. The presence of the hydrogel improved the linear dynamic range but reduced sensitivity and response time. This could be due to the enzyme loading in the PPy-hydrogel and/or to the diffusion limitation of glucose through the interpenetrating network of PPy within the hydrogel. The observed difference in response time would have no practical impact on performance. Both polypyrrole and the hydrogel are shown to have an effect on enzyme affinity and stability [39,40]. The apparent Michaelis–Menten constant K_M and the maximum current response, I_{max}, were calculated from the slope and the intercept of the Lineweaver–Burk plots [41,42].

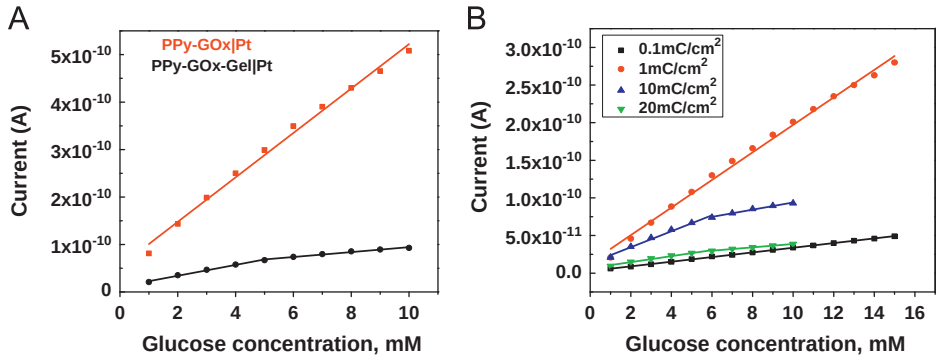

Fig. 4. Glucose dose-response curves of biotransducers (ϕ=100 μm) PPy–GOx–Pt (red) and PPy–GOx-Gel–Pt composite membrane (black). (A) A comparison of PPy–GOx–Pt (red) and PPy-GOx-Gel–Ptat 10 mC/cm^2 and (B) a comparison of PPy–GOx-Gel–Pt at various electropolymerization charges. (For interpretation of the references to color in this figure legend, the reader is referred to the web version of this article.)

Table 1
Bioanalytical performance of PPy-GOx–Pt and PPy-GOx-Gel–Pt biotransducers as a function of electropolymerization charge density measured after 7 days of storage in PBS 7.2 at 4 °C.

	PPy–GOx–Pt	PPy–GOx-Gel–Pt				
Charge density (mC/cm^2)	10	0.1	1	10	20	100
S (nA/mM/cm^2)	596 (1–10 mM)	39 (1–15 mM)	281 (1–15 mM)	146 (1–6 mM) 61 (6–10 mM)	84 (1–6 mM) 29 (6–10 mM)	45 (1–5 mM) 6 (8–33 mM)
Linear dynamic range (mM)	1–10 –	1–15 –	1–15 –	1–6 6–10	1–6 6–10	1–5 8–33
Response time (s)	20	20	50	50	70	2–8
Detection limit (mM)	0.004	0.621	0.033	0.020	0.030	0.098
K_M (mM)	11.65	29.2	33	6	4.6	0.57
I_{max} (μA/cm^2)	12.7	1.7	13.2	1.9	0.7	0.6

For PPy–GOx-Gel composite K_M=11.4 mM and I_{max}=3.3 μA/cm^2 and for PPy–GOx composite K_M=7.6 mM and I_{max}=9.1 μA/cm^2. In both cases the value of the K_M was higher than that independently determined using spectrophotometry in solution (K_M=6 mM).

3.4. *Effect of electropolymerization charge on the response of PPy–GOx-Gel|Pt*

The charge density dependence of electropolymerized PPy on the sensitivity of the biotransducer was examined. After 7 days of storage at 4.0 °C in PBS 7.2 buffer, the sensitivity of 0.1, 1, 10, 20, and 100 mC/cm^2 current densities used for GOx immobilization onto biotransducers were compared. Biotransducers with charge densities ranging from 0.1 to 20 mC/cm^2 were prepared on a platinum microelectrode and the biotransducer with a charge density of 100 mC/cm^2 was prepared using a microdisc electrode array that has previously been reported [9,43]. Amperometric responses were normalized to electrode surface area. The linear dynamic range was shown to be influenced by the charge density. Increasing the total charge density decreased the effective linear dynamic range. Improved linear range has previously been attributed to higher porosity of low charge densitypolypyrrole [44]. Increasing the overall applied charge density led to an increase in the response time of biotransducers. This result was expected as additional polypyrrole will lead to a decrease in permeability of the bioactive membrane [45]. Average pore radius of mesoporous polypyrrole films has been shown to be approximately 17–19 Å [46]. Low charge densities of electropolymerized polypyrrole have been observed to have higher specific capacitances which subsequently decrease with further applied charge density [47]. For polypyrrole systems, higher specific capacitances are attributed to higher porosity networks that increase permeability of electrolytes through the mesopores [48]. Blockage of these nano-features may result due to the overgrowth of polypyrrole [21,49]. Other findings have shown that increasing polypyrrole charge density decreases response time of the amperometric biosensor, but no explanation was proposed as to why this may be occurring [45].

We observed an initial rise followed by a decrease in sensitivity with the maximum sensitivity being observed at 1 mC/cm^2, Fig. 5. Very similar trends have been observed for cholesterol oxidase and glucose oxidase biotransducers fabricated with over-oxidized polypyrrole [45,50,51]. Decreases to sensitivity have been attributed to decreases in permeability of hydrogen peroxide as polypyrrole thickness increases [50]. Polypyrrole film morphology is highly dependent upon the electropolymerization charge density [52] and as a result may be having more influence on the activity of the enzymes. Thicker polypyrrole layers also allow more enzymatic reactions to take place closer to the solution/bioactive-membrane interface with subsequent diffusion of hydrogen peroxide into bulk solution rather than to the surface of the transducer [50,51,53].

Fructose dehydrogenase immobilized by polypyrrole has also been shown to have a maximum amperometric current response at a charge density of 1 mC/cm^2 for fructose biosensors [54]. The inflection of maximum sensitivity for glucose was at a lower PPy charge density or thickness when compared to some other findings [55,56]. This indicates that PPy generated within the pHEMA hydrogel reaches saturating levels more quickly than PPy deposited directly onto electrodes, consistent with previously reported findings [57]. Incorporation of the hydrogel diminishes sensitivity by a factor of four and increases the response time by a factor of two. This was shown to be the case at a charge density of 10 mC/cm^2 for PPy–GOx electrodes which had a sensitivity of

596 nA/mM/cm^2 when compared to PPy–GOx-Gel electrodes having a sensitivity of 146 nA/mM/cm^2, Table 1. Polypyrrole based enzyme immobilization onto bare electrodes does not typically reach diffusion limiting levels until polymer thickness reaches >250 nm or a charge density of >100 mC/cm^2 indicating that the hydrogel has an appreciable influence on biosensor performance [53,58].

The hydrogel utilized was crosslinked with 3 mol% TEGDA, making it a highly tortuous network even prior to the formation of the interpenetrating network of PPy [59]. It has been shown that the void volume and tortuosity increase dramatically by increasing crosslink density of pHEMA hydrogels [60]. This can lead to both decreased diffusivity of hydrogen peroxide. Loss of enzyme activity due to the immobilization process cannot be ruled out. For the lower charge densities K_{Mapp} equals approximately the Michaelis–Menten coefficients for GOx in solution [61]. The amount of polypyrrole incorporated into the hydrogels may be influencing the bound to free water ratio which can account for the observed trend in K_{Mapp}. Bound water has been shown to decrease in similar hydrogel systems with increasing TEGDA crosslink density [59]. We observed that the overall enzyme activity decrease for charge densities >1 mC/cm^2 but increased in apparent substrate affinity.

It is clear that optimizations will require choosing the combination of cross-link density and electropolymerization charge density that achieves the best sensitivity, linear dynamic range and lowest detection limit. For example, the crosslink density (mol% TEGDA) may be decreased to accommodate interpenetrating network formation via pyrrole electropolymerization. The systems design of an implantable amperometric biosensor in this body of work has shown to have predictable properties based on electropolymerization of polypyrrole. One of the major drawbacks is the decrease in sensitivity of biotransducers formed from PPy–GOx-Gel composites. Even so, there are appreciable added benefits in using a PPy-hydrogel composite for biosensing purposes. The PPy-hydrogel composites have been shown to have superior cell viability *in vitro* compared to PPy or hydrogel alone [62]. Other studies have shown polypyrrole to be positively biocompatible with central nervous tissues [63] and peripheral nervous tissues [64] and polypyrrole particles have been shown to not illicit inflammation to peritoneal cells after a 6-week period [65].

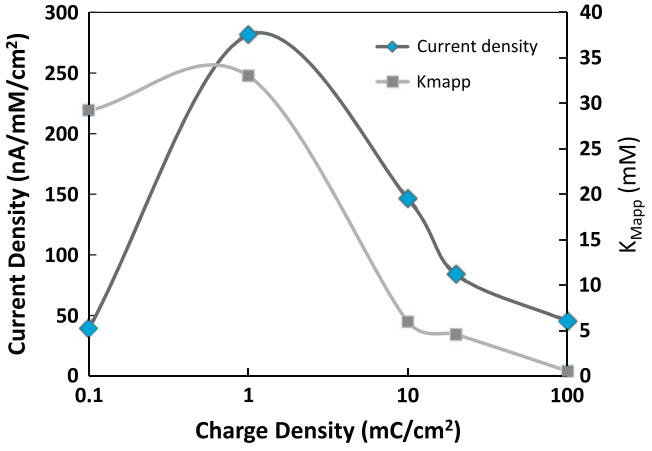

Fig. 5. Trends in the amperometric current density for 5 mM glucose and the apparent Michaelis–Menten enzyme affinity constant, K_{Mapp}, as a function of electropolymerization charge density (mC/cm^2). The charge density of100 mC/cm^2 was determined using a microelectrode array.

3.5. Ascorbic acid interference and effects of the applied potential

Ascorbic acid (AA) is a negatively charged endodgenous interferent that is known to perturb biosensor response *in vivo*. Ascorbic acid, along with other negatively charged, redox-active interferents must be screened in order to prevent their non-specific oxidation. Failure to take this into account may lead to significant errors during *in vivo* sensing. A relevant range of oxidative potentials for the oxidation of hydrogen peroxide was examined using a hydrogel coated, 10 mC/cm^2 PPy biotransducer. It was noted that for a clinically relevant concentration of AA [66] only 3–5% of the total current response was contributed by AA at the low concentration of 5 mM glucose, Fig. 6. Even at the highest applied potential of 700 mV the biotransducer maintained a reasonable screening ability.

Polypyrrole is known for its interferent screening capability by anion exclusion after over oxidation thereby preventing the diffusion of negatively charged ascorbic acid, uric acid, and acetaminophenol [34,67]. Polypyrrole used with similar hydrogel systems have been able to suppress interferents of ascorbic acid and L-cysteine at twice the physiological levels found in serum by maintaining their deviations to less than 5% of a glucose responsive biosensor [68]. Polypyrrole shows a consistency in its screening ability for interferents in bioactive pHEMA-based hydrogel membranes. Thicker polypyrrole layers with less incorporated enzyme will have the drawback of decreased sensitivity and linear range but increased screening capability of interferents [69].

3.6. Time dependence of performance—stability

Fig. 7 shows the amperometric response of two biotransducers (1.0 and 10 mC/cm^2) observed over time. An overall trend of increasing biotransducer sensitivity as a function of storage time was noted. The biotransducer of 1.0 mC/cm^2 plateaued at approximately 21 pA/mM after 15 days of storage. The biotransducer at

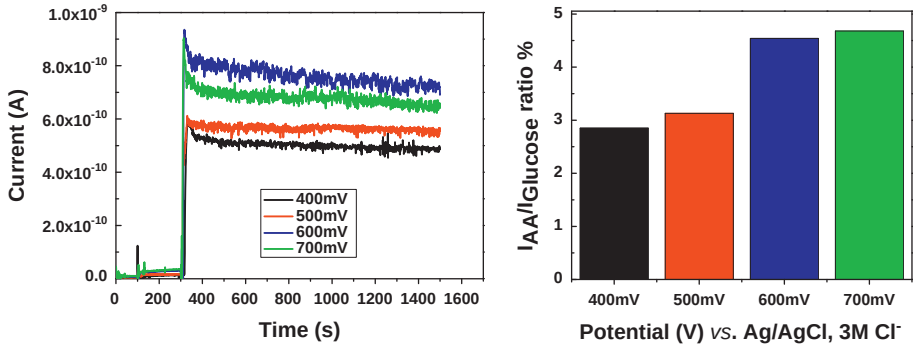

Fig. 6. Glucose dose-response curves of biotransducers ($\phi=100$ μm) PPy0–GOx –Pt (red) and PPy–GOx-Gel–Pt composite membrane (black). (A) A comparison of PPy–GOx–Pt (red) and PPy–GOx-Gel–Pt at 10 mC/cm^2 and (B) A comparison of PPy–GOx-Gel–Pt at various electropolymerization charges. (For interpretation of the references to color in this figure legend, the reader is referred to the web version of this article.)

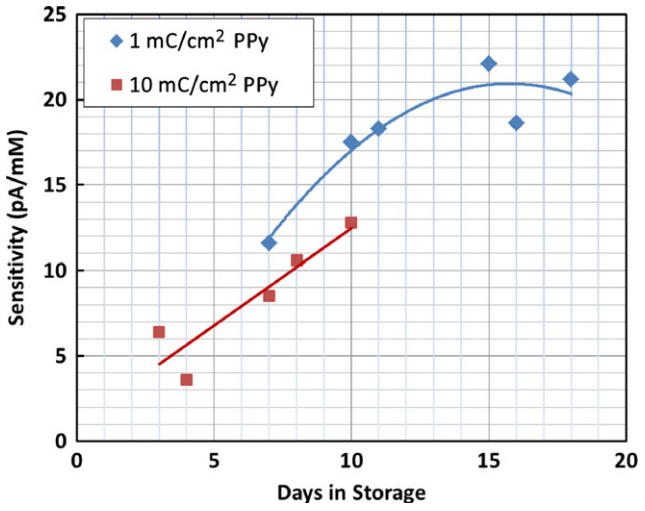

Fig. 7. Temporal changes in the sensitivity of stored PPy–GOx-Gel–Pt biotransducers prepared with 1 and 10 mC/cm^2 as a function of days of storage in PBS 7.2 at 4 °C.

10 mC/cm^2 had a similar trend but was not observed beyond 10 days of storage. The most dramatic changes in stability of PPy–GOx biosensors have been shown to occur within the first 5 days of storage [56]. Typically biotransducers are characterized by a decrease in sensitivity and maximum current with increasing storage time [70]. Amperometric biotransducers utilizing PPy have been shown to have 21 days of stability but a very sharp decrease in sensitivity thereafter [22]. Ideally no changes to sensitivity or maximum current should occur over time. Stability of up to 20 days, with no changes in sensitivity, has been observed for PPy–GOx systems using electrochemical surface plasmon resonance [71]. Given proper calibration, the stability of the polypyrrole based enzyme amperometric biosensors have a reasonably long lifetime of use. Polypyrrole has been shown to protect enzymes from leaching out in some cases as well as protecting and stabilizing their activity [36,37,72]. It is uncertain as to why a maturation process occurs for the investigated PPy–GOx-Gel composite biotransducers. One possibility is that hydration of the polypyrrole matrix is occurring over time. The applied potential of 400 mV *vs.* Ag/AgCl during interrogation is believed to be high enough to induce degradation of polypyrrole [73], however, the polypyrrole of the current biotransducers are already over oxidized. There is the possibility of some partial enzyme unfolding during electro-immobilization that may be accompanied by refolding within the hydrogel during storage leading to more of the entrapped enzymes to become active, increasing the enzyme efficiency of the biotransducer. Experimental determination of enzyme secondary structure using FT-IR and circular dichroism may be performed in the future to determine if this is the case.

4. Conclusions

It is highly feasible to fabricate amperometric enzyme biotransducers using the procedure of Py electropolymerization to ensnare GOx and immobilize it within hydrogel membrane layers that were covalently anchored onto surface modified platinum electrodes. Cyclic voltammetry showed that surface modification using APTMS compromises electroactivity and the hydrogel membrane layer compromises biotransducer sensitivity. The electropolymerization charge density dependence of biotransducer sensitivity and enzyme activity revealed a maximum sensitivity of 281 nA/mM/cm^2 around 1.0 mC/cm^2 and an apparent K_M of 33 mM. Screening of ascorbic acid was consistent with previously reported results. A temporal improvement in biotransducer sensitivity, regardless of charge density of fabrication, was associated with the presence of the hydrogel membrane layer. Such increases in sensitivity indicate increases in immobilized enzyme activity over time. There is need to investigate and optimize the relationship between the crosslink-density and the electopolymerization charge density in order to achieve a strategic balance been the compromise in sensitivity and the benefits of interference screening, biocompatibility and long term enzyme stability.

Novelty statement

Electropolymerization of pyrrole in the presence of glucose oxidase and within electrode-supported hydrogels yields biotransducers that show improvement in sensitivity upon storage.

Acknowledgments

This work was supported by the US Department of Defense (DoDPRMRP) grant PR023081/DAMD17-03-1-0172, by the Consortium of the Clemson University Center for Bioelectronics, Biosensors and Biochips (C3B) and by ABTECH Scientific, Inc.

References

[1] C.N. Kotanen, F.G. Moussy, S. Carrara, A. Guiseppi-Elie, Biosens. Bioelectron. 35 (2012) 14–26.
[2] J. Wang, Chem. Rev. 108 (2008) 814–825.
[3] A. Guiseppi-Elie, in: Anthony Guiseppi-Elie (Ed.), USPTO, USA, 2011.
[4] A. Guiseppi-Elie, Anal. Bioanal. Chem. 399 (2011) 403–419.
[5] A. Thorell, J. Nygren, O. Ljungqvist, Curr. Opin. Clin. Nutr. Metab. Care 2 (1999) 69–78.
[6] Y. Ma, B. Toth, A.B. Keeton, L.T. Holland, I.H. Chaudry, J.L. Messina, Endocrinology 145 (2004) 5168–5176.
[7] J. Xu, H.T. Kim, Y. Ma, L. Zhao, L. Zhai, N. Kokorina, P. Wang, J.L. Messina, Endocrinology 149 (2008) 2369–2382.
[8] L. Li, L.H. Thompson, L. Zhao, J.L. Messina, Endocrinology 150 (2009) 24–32.
[9] A.R.A. Rahman, G. Justin, A. Guiseppi-Elie, Biomed. Microdevices 11 (2009) 75–85.
[10] G. Fu, X. Yue, Z. Dai, Biosens. Bioelectron. 26 (2011) 3973–3976.
[11] C. Kotanen, A. Guiseppi-Elie, Macromol. Symp. (2012).
[12] S. Bourigua, S.E. Ichi, H. Korri-Youssoufi, A. Maaref, S. Dzyadevych, N.J. Renault, Biosens. Bioelectron. (2011).
[13] Z. Zhang, Y. Xie, Z. Liu, F. Rong, Y. Wang, D. Fu, J. Electroanal. Chem. 650 (2011) 241–247.
[14] S.B. Adeloju, A.T. Lawal, Anal. Chim. Acta 691 (2011) 89–94.
[15] K.Y. Kwon, J. Youn, J.H. Kim, Y. Park, C. Jeon, B.C. Kim, Y. Kwon, X. Zhao, P. Wang, B.I. Sang, J. Lee, H.G. Park, H.N. Chang, T. Hyeon, S. Ha, H.-T. Jung, J. Kim, Biosens. Bioelectron. 26 (2010) 655–660.
[16] M. Kato, H. Saruwatari, K. Sakai-Kato, T. Toyo'oka, J. Chromatogr. A 1044 (2004) 267–270.
[17] K. Molvinger, F. Quignard, D. Brunel, M. Boissière, J.-M. Devoisselle, Chem. Mater. 16 (2004) 3367–3372.
[18] T. Coradin, J. Livage, So–Gel Synthesis of Solids, in: Encyclopedia of Inorganic Chemistry, John Wiley & Sons, Ltd., 2006.
[19] J. Yan, V.A. Pedrosa, A.L. Simonian, A. Revzin, ACS Appl. Mater. Interfaces 2 (2010) 748–755.
[20] C. Apetrei, M. Rodríguez-Méndez, J. De Saja, Electrochim. Acta (2011).
[21] M.P. Massafera, S.I.C. de Torresi, Electroanalysis 23 (2011) 2534–2540.
[22] A. Kausaite-Minkstimiene, V. Mazeiko, A. Ramanaviciene, A. Ramanavicius, Sens. Actuators B 158 (2011) 278–285.
[23] A. Guiseppi-Elie, S. Brahim, D. Narinesingh, J. Macromol. Sci.—Pure Appl. Chem. A38 (2001) 1575–1591.
[24] S. Brahim, D. Narinesingh, A. Guiseppi-Elie, Macromol. Symp. 186 (2002) 63–73.
[25] G. Justin, A. Guiseppi-Elie, J. Bioactive Compatible Polym. 25 (2010) 121–140.
[26] C. Kotanen, C. Tlili, A. Guiseppi-Elie, Appl. Biochem. Biotechnol. 166 (2012) 878–888.
[27] S. Abraham, S. Brahim, K. Ishihara, A. Guiseppi-Elie, Biomaterials 26 (2005) 4767–4778.
[28] C. Kotanen, A. Guisepp-Elie, Am. Soc. Gravitational Space Biol. Bull. 23 (2010) 55–63.
[29] A. Guiseppi-Elie, A.M. Wilson, J.M. Tour, T.W. Brockmann, P. Zhang, D.L. Allara, Langmuir 11 (1995) 1768–1776.
[30] S.B. Hall, E.A. Khudaish, A.L. Hart, Electrochim. Acta 43 (1997) 579–588.

[31] P. Pandey, S. Upadhyay, I. Tiwari, V. Tripathi, Sens. Actuators B 72 (2001) 224–232.
[32] N.C. Foulds, C.R. Lowe, Anal. Chem. 60 (1988) 2473–2478.
[33] K. Itaya, N. Shoji, I. Uchida, J. Am. Chem. Soc. 106 (1984) 3423–3429.
[34] S. Brahim, D. Narinesingh, Anthony Guiseppi-Elie, Electroanalysis 14 (2002) 627–633.
[35] J. Wang, M. Musameh, Anal. Chim. Acta 539 (2005) 209–213.
[36] G. Fortier, E. Brassard, D. Bélanger, Biosens. Bioelectron. 5 (1990) 473–490.
[37] G. Fortier, D. Bélanger, Biotechnol. Bioeng. 37 (1991) 854–858.
[38] J. Morais, F. Papadimitrakopoulos, D. Burgess, AAPS J. 12 (2010) 188–196.
[39] S. Brahim, D. Narinesingh, A. Guiseppi-Elie, Biosens. Bioelectron. 17 (2002) 973–981.
[40] S. Brahim, D. Narinesingh, A. Guiseppi-Elie, J. Mol. Catal. B: Enzymatic 18 (2002) 69–80.
[41] J. Yu, S. Liu, H. Ju, Biosens. Bioelectron. 19 (2003) 401–409.
[42] R.A. Kamin, G.S. Wilson, Anal. Chem. 52 (1980) 1198–1205.
[43] A. Guiseppi-Elie, Macromolecular Symposia 317 (2012) 187–197.
[44] S.B. Adeloju, A.N. Moline, Biosens. Bioelectron. 16 (2001) 133–139.
[45] Y.-C. Tsai, S.-C. Li, S.-W. Liao, Biosens. Bioelectron. 22 (2006) 495–500.
[46] A. Hallik, A. Alumaa, H. Kurig, A. Jänes, E. Lust, J. Tamm, Synthet. Met. 157 (2007) 1085–1090.
[47] L.Z. Fan, J. Maier, Electrochem. Commun. 8 (2006) 937–940.
[48] K. Rajendra Prasad, N. Miura, Electrochem. Commun. 6 (2004) 849–852.
[49] K. Noh, D.W. Kim, C.S. Jin, K.H. Shin, J.H. Kim, J.M. Ko, J. Power Sour. 124 (2003) 593–595.
[50] J.C. Vidal, E. Garcı´a, J.R. Castillo, Anal. Chim. Acta 385 (1999) 213–222.
[51] Y. Kajiya, H. Sugai, C. Iwakura, H. Yoneyama, Anal. Chem. 63 (1991) 49–54.
[52] R. Valaski, S. Ayoub, L. Micaroni, I.A. Hümmelgen, Thin Solid Films 415 (2002) 206–210.
[53] P. Gros, A. Bergel, J. Electroanal. Chem. 386 (1995) 65–73.
[54] M.J. Swann, D. Bloor, T. Haruyama, M. Aizawa, Biosens. Bioelectron. 12 (1997) 1169–1182.
[55] W.J. Sung, Y.H. Bae, Biosens. Bioelectron. 18 (2003) 1231–1239.
[56] N.F. Almeida, E.J. Beckman, M.M. Ataai, Biotechnol. Bioeng. 42 (1993) 1037–1045.
[57] G. Justin, A. Guiseppi-Elie, Biomacromolecules 10 (2009) 2539–2549.
[58] F. Palmisano, C. Malitesta, D. Centonze, P.G. Zambonin, Anal. Chem. 67 (1995) 2207–2211.
[59] A.N. Wilson, R. Salas, A. Guiseppi-Elie, J. Controlled Release 160 (2012) 41–47.
[60] C. Kotanen, A.N. Wilson, A.M. Wilson, K. Ishihara, A. Guiseppi-Elie, Biomed. Microdevices 14 (2012) 549–558.
[61] N.C. Foulds, C.R. Lowe, J. Chem. Soc. Faraday Trans. 1 (82) (1986) 1259–1264.
[62] A. Guiseppi-Elie, Biomaterials 31 (2010) 2701–2716.
[63] P.M. George, A.W. Lyckman, D.A. LaVan, A. Hegde, Y. Leung, R. Avasare, C. Testa, P.M. Alexander, R. Langer, M. Sur, Biomaterials 26 (2005) 3511–3519.
[64] X. Wang, X. Gu, C. Yuan, S. Chen, P. Zhang, T. Zhang, J. Yao, F. Chen, G. Chen, J. Biomed. Mater. Res. A 68A (2004) 411–422.
[65] A. Ramanaviciene, A. Kausaite, S. Tautkus, A. Ramanavicius, J. Pharm. Pharmacol. 59 (2007) 311–315.
[66] J. Moran, L. Cohen, J. Greene, G. Xu, E. Feldman, C. Hames, D. Feldman, Am. J. Clin. Nutr. 57 (1993) 213–217.
[67] J. Rubio Retama, E. López Cabarcos, D. Mecerreyes, B. López-Ruiz, Biosens. Bioelectron. 20 (2004) 1111–1117.
[68] S. Brahim, D. Narinesingh, A. Guiseppi-Elie, Anal. Chim. Acta 448 (2001) 27–36.
[69] M.C. Shin, H.S. Kim, Anal. Lett. 28 (1995) 1017–1031.
[70] J. Shi, P. Ci, F. Wang, H. Peng, P. Yang, L. Wang, S. Ge, Q. Wang, P.K. Chu, Biosens. Bioelectron. 26 (2011) 2579–2584.
[71] L. Tian, J. Qiu, Y.-C. Zhou, S.-G. Sun, Microchim. Acta 169 (2010) 269–275.
[72] J. Njagi, S. Andreescu, Biosens. Bioelectron. 23 (2007) 168–175.
[73] H. Yamato, M. Ohwa, W. Wernet, J. Electroanal. Chem. 397 (1995) 163–170.